

Spatiotemporal shaping of terahertz pulses

Jake Bromage, Stojan Radic, G. P. Agrawal, and C. R. Stroud, Jr.

The Institute of Optics, University of Rochester, Rochester, New York 14627

P. M. Fauchet and Roman Sobolewski

Department of Electrical Engineering and Laboratory for Laser Energetics, University of Rochester, Rochester, New York 14627

Received January 10, 1997

We report temporal shaping of few-cycle terahertz pulses, using a slit in a conductive screen as a high-pass filter. The filter's cutoff frequency was tuned by changing the width of the slit; the slope of the cutoff transition was altered by changing the thickness of the screen. We measured the transmission function of the filters, using large-aperture photoconducting antennas to create and detect the incident and transmitted electric field. Our experimental results were in excellent agreement with the performed finite-difference time-domain simulations of the propagation of the pulse through the slit. When the screen thickness was greater than the slit width, the filter was well modeled by a short, planar waveguide. Using a simple transfer function, we accurately describe the sharp cutoff and dispersion of such a filter. © 1997 Optical Society of America

Recently terahertz (THz) pulses have proved useful for a wide variety of applications, including far-infrared^{1/} time-domain spectroscopy,² study and control of Rydberg atoms,³ T-ray imaging of optically opaque materials,⁴ and impulse-ranging studies.⁵ Applications exploit the features of THz pulses that distinguish them from optical pulses, namely their broad bandwidth and long center wavelength. The broad bandwidth allows for the exciting possibility for sculpting the pulses to meet a desired goal by modifying their spectra. Although shaped THz pulses have been made by modifying the optical pump intensity profile⁶ or by manufacturing more complex emitters,⁷ there are advantages to sculpting the THz field directly.^{8,9} Because of the long wavelengths, fabricating quasi-optical components for THz pulses is easier than for optical pulses. Further, we can directly characterize the effect of the THz shaping elements on the pulse, using sampling techniques to measure the electric field rather than the intensity.

In this Letter we report experiments in which we shaped THz pulses using a slit in a conductive screen as a high-pass filter.¹⁰ We show that the shape of the electric-field pulse transmitted through such a slit filter depends on the slit width and the screen thickness. The filter's high-pass cutoff frequency, ν_c , is inversely proportional to the slit width, d , and so it can easily be tuned. Varying the screen thickness, l , leads to two modes of operation: If the screen thickness of the filter is much less than the cutoff wavelength, the filtering results from lower frequencies' diffracting more severely. On the other hand, if the filter's thickness is greater than the cutoff wavelength, the filter behaves like a short planar waveguide. This produces a much sharper cutoff transition and pulse dispersion, which we describe with a simple transfer function. We also show the highly accurate results of finite-difference time-domain (FDTD) simulations of pulses propagating through both types of slit filter.

The experimental configuration is shown in Fig. 1. Both the emitter and detector of the THz

radiation were large-aperture photoconductive antennas.¹¹ We made the emitter of 1-cm^2 $\langle 100 \rangle$ semi-insulating GaAs biased with a field of 2 kV/cm via parallel Au-Ge-Ni electrodes. A 150-fs, 810-nm Ti:sapphire optical pulse triggered the THz emission by uniformly illuminating the GaAs wafer with a fluence of $20\text{ }\mu\text{J/cm}^2$. We fabricated the detector by depositing parallel Au-Ge-Ni electrodes, spaced 2 mm apart, upon an epilayer of low-temperature molecular-beam-epitaxy-grown GaAs (LT-GaAs). The $1.5\text{-}\mu\text{m}$ -thick LT-GaAs layer was grown at 200°C and annealed *in situ* at 600°C to produce a short carrier lifetime of $\sim 1\text{ ps}$. A delayed Ti:sapphire pulse gated the detector by uniformly illuminating the 2-mm^2 active area with a fluence of 0.5 mJ/cm^2 . When the optical and the THz pulses were present in the LT-GaAs at the same time, the carriers produced by the optical pulse were accelerated by the electric field of the THz pulse. The component of the THz field perpendicular to the detector electrodes caused a current to flow in an external circuit. We measured this small current ($\sim 1\text{ pA}$) by chopping the 1-kHz optical pulse train that triggers the emitter and using a lock-in amplifier. By varying the delay between the arrival of the THz pulse and the optical gating pulse at the detector,

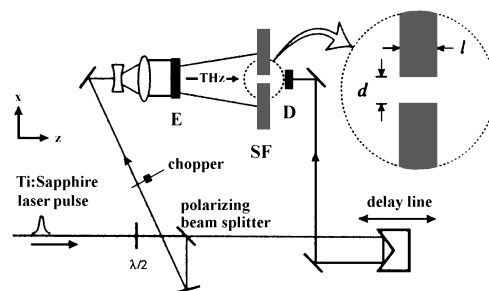


Fig. 1. Schematic of the experimental setup showing the THz emitter (E), the dimensions of the slit filter (SF), and the detector (D). The THz radiation is polarized along the y axis.

one can sample the THz pulse electric field with a resolution that depends on the lifetime of the carriers in the LT-GaAs. The shortest feature resolved by the detector has a duration of ~ 600 fs.

The adjustable slit filter was formed between the edges of two $5\text{ cm} \times 10\text{ cm}$ sheets of copper, oriented parallel to the direction of THz polarization. The slit was 10 cm from the emitter, ensuring an approximately planar wave front over the slit widths of interest (0.1–5 mm). The incident THz pulse shown in Fig. 2 was measured 7 mm in front of the slit. Its main peak has a width (FWHM) of 1.3 ps and contains 72% of the detected energy. The small feature ~ 12 ps after the main peak is due to reflections within the 0.5-mm-thick emitter. The power spectrum of the pulse is peaked at 0.2 THz and extends past 1 THz.

We measured the effect of two types of slit filter: the thickness of the screen, l , was either much less than or greater than the cutoff wavelength. To make a slit filter in a screen whose thickness l is much less than the shortest wavelength of the THz pulse ($1\text{ THz} \equiv 300\ \mu\text{m}$), we mounted razor blades on the inner edges of the copper sheets. To make a thick filter (i.e., a slit in a thick screen), we used a slit formed between 1.7-mm-thick copper sheets. By adjusting the slit width, d , we changed the shape of the transmitted pulses measured 7 mm after the filter. For slit widths $d \sim 1\text{ mm}$, the pulses transmitted by the thick and thin filters are dramatically different, as shown in Fig. 3. Note that the pulse transmitted by the thick filter is chirped and oscillates with a period that decreases as the slit width decreases.

To verify our experimental findings, we numerically simulated the propagation of the THz pulse through the slit, using the FDTD method¹² with a spatial resolution of $15\ \mu\text{m}$ ($< \lambda/20$) and a temporal resolution of 25 fs. We modeled the copper screen as a perfect conductor by requiring that the tangential component of the electric field vanish on its surface. (Note that the skin depth of copper at THz frequencies is $\sim 5\ \mu\text{m}$ —much less than the wavelength.) To facilitate direct comparison of experiments and simulations, we used actual experimental parameters together with the measured input field as the starting point for the simulations. Figure 3 shows the agreement between the experiments and the simulations. Note that no fitting parameters were used. These highly accurate simulations allow us to examine the pulse in regions where we cannot directly measure it and to test more complicated filter structures.

The performance of the slit filters is easiest to analyze in the frequency domain. We calculated the experimental transfer functions for the filters, $T(\nu) = \tilde{E}_{\text{out}}(\nu)/\tilde{E}_{\text{in}}(\nu)$, over the bandwidth of the incident pulse [$\tilde{E}(\nu)$ is the Fourier transform of the field, $E(t)$, measured at the input or output of the filter]. The magnitude and phase of $T(\nu)$ for the thin and thick filters are shown in Fig. 4. Both filters had a slit width of $d = 0.5\text{ mm}$. For the thin filter, the high pass rolled off at $\sim 0.3\text{ THz}$ and the 6-dB width of the transition band was 137 GHz. The phase was linear over a large portion of the transmitted bandwidth, and thus there was little dispersion. On the other hand,

for the thick filter ($l = 1.7\text{ mm}$), there was a sharp cutoff at 0.30 THz with a 6-dB transition bandwidth of 37 GHz. Further, the phase was not linear near the cutoff frequency, which accounts for the observed dispersion. This is to be expected as the magnitude and phase of a passive filter transfer function are related by Hilbert transforms; a sharp transmission cutoff implies dispersion.¹³

The transfer function for a slit in an infinitesimally thin, perfectly conducting screen has been calculated.^{14,15} Comparison between this result and the experimental $|T(\nu)|$ for the thin filter shows good qualitative agreement; the location of the roll-off is at the predicted $\nu_r \approx 1.5c/\pi d$, and the transmission below falls off slowly to zero with the frequency. For the

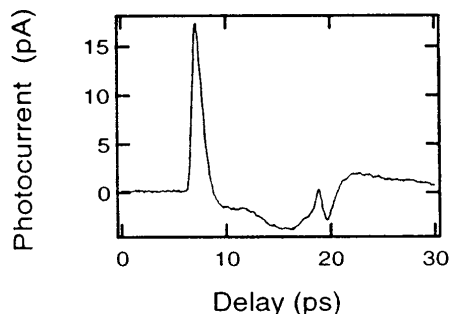


Fig. 2. THz pulse shape measured before the slit filter.

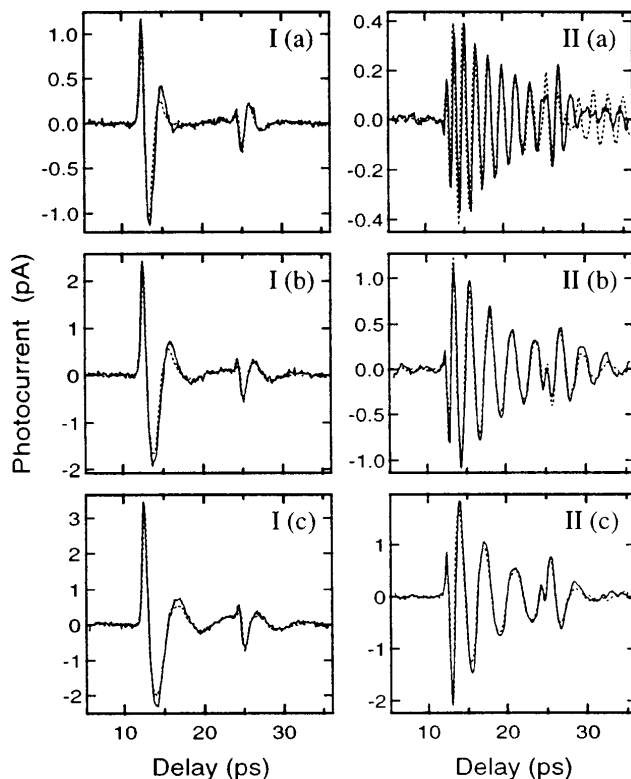


Fig. 3. Measured and calculated output of the slit filters. Column I is the thin-filter output; column II is the thick-filter output. The slit widths are (a) $300\ \mu\text{m}$, (b) $500\ \mu\text{m}$, and (c) $700\ \mu\text{m}$. The solid curves are measured signals; the dashed curves are the results of the FDTD simulations.

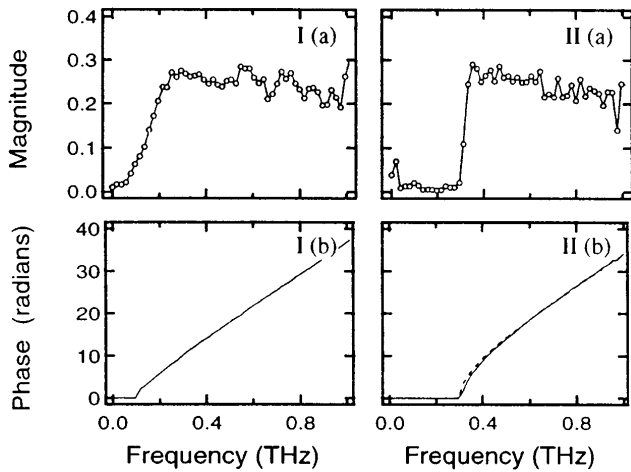


Fig. 4. Measured slit filter transfer functions for $d = 500 \mu\text{m}$. Column I is for the thin-filter transfer function; column II is for the thick filter. The dashed curve in II (b) shows the phase predicted by the waveguide model.

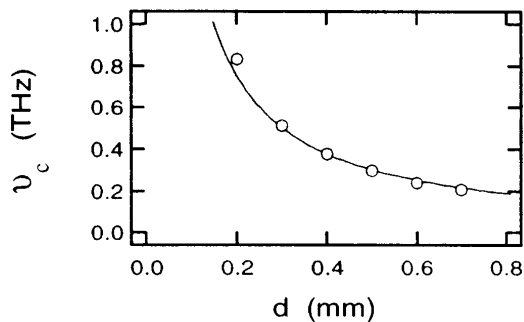


Fig. 5. Thick-filter cutoff frequency ν_c versus the slit width d . The points are the measured cutoff frequencies; the solid curve is the waveguide model prediction.

thin filters, the filtering results from the more severe diffraction at lower frequencies.

The transfer function for the thick filter can be described by the simple single-mode model of a short, planar waveguide. Formed between the parallel faces inside the slit, the waveguide has a width d and a length l . The modes of the waveguide have a propagation constant

$$\beta(\nu) = \begin{cases} \frac{\pi}{d} \sqrt{(\nu/\nu_c)^2 - 1} & \text{if } \nu > \nu_c \\ i \frac{\pi}{d} \sqrt{1 - (\nu/\nu_c)^2} & \text{if } \nu \leq \nu_c \end{cases},$$

where $\nu_c = c/2d$ is the cutoff frequency. The transfer function is $T(\nu) = \exp[i\beta(\nu)l]$. For frequencies above ν_c , β is real and thus the mode propagates without loss; for frequencies below ν_c , β is imaginary and the mode is evanescent. If the length l of the waveguide is longer than the cutoff wavelength, the power at frequencies below ν_c will be strongly attenuated, causing the waveguide to work as a high-pass filter. In Fig. 4, the phase of the waveguide transfer function is compared with the phase of the transfer function for the thick filter with the same d . To permit direct comparison, we set the time

delay between the input and output experimental traces equal to the free-space propagation time for the 1.7-mm waveguide length. In Fig. 5, the experimentally determined cutoff frequency is compared with the cutoff of the waveguide for a range of d . Note that the thick filter severely attenuates low frequencies that are passed by the thin filter. At the 6-dB frequency of the thin filter the attenuation of the thick filter is 37 dB. Thus the characteristics of the thick filter are determined predominantly by the waveguide cutoff and not by subsequent diffraction. The severe diffraction could be reduced with silicon lenses similar to those used to collimate the THz radiation emitted by photoconductive dipole antennas.

Finally, we also examined the case in which the THz pulse was polarized orthogonal to the slit edges. The experiment and FDTD simulations were in excellent agreement, and we found no shaping of the transmitted pulse shape. This is to be expected, as there are no waveguide modes for this polarization.

We thank G. Wicks for providing the LT-GaAs samples and acknowledge helpful discussions with L. Casperson, J. West, and J. D. Corless. This research was supported by the U.S. Army Research Office and by the National Science Foundation under contract ECS-9413989.

References

1. D. Grischkowsky, S. Keiding, M. van Exter, and C. Fattinger, *J. Opt. Soc. Am. B* **7**, 2006 (1990).
2. S. R. Keiding, *Comm. At. Mol. Phys.* **30**, 37 (1994).
3. R. R. Jones, *Phys. Rev. Lett.* **76**, 3927 (1996).
4. B. B. Hu and M. C. Nuss, *Opt. Lett.* **20**, 1716 (1995).
5. R. A. Chevillat and D. Grischkowsky, *Appl. Phys. Lett.* **67**, 1960 (1995).
6. A. S. Weling, B. B. Hu, N. M. Froberg, and D. H. Auston, *Appl. Phys. Lett.* **64**, 137 (1994).
7. N. M. Froberg, B. B. Hu, X.-C. Zhang, and D. H. Auston, *IEEE J. Quantum Electron.* **28**, 2291 (1992).
8. J. O. White, C. Ludwig, and J. Kuhl, *J. Opt. Soc. Am. B* **12**, 1687 (1995).
9. R. H. Garnham, in *Millimetre and Submillimetre Waves*, F. A. Benson, ed. (Iliffe, London, 1969), Chap. 21, pp. 403–450.
10. Apertures have been used as high-pass filters for detector characterization in W. Sha, T. B. Norris, J. W. Burm, D. Woodard, and W. J. Schaff, *Appl. Phys. Lett.* **61**, 1763 (1992).
11. J. T. Darrow, D. H. Auston, and J. D. Morse, *Proc. SPIE* **1861**, 186 (1993).
12. A. Taflove, *Computational Electrodynamics: The Finite Difference Time-Domain Method* (Artech, Boston, Mass., 1995).
13. D. S. Humpherys, *The Analysis, Design, and Synthesis of Electrical Filters* (Prentice-Hall, Englewood Cliffs, N.J., 1970), pp. 68–77.
14. P. M. Morse and P. J. Rubinstein, *Phys. Rev.* **54**, 895 (1938).
15. J. S. Asvestas and R. E. Kleinman, in *Electromagnetic and Acoustic Scattering by Simple Shapes*, J. J. Bowman, T. B. A. Senior, and P. L. E. Uslenghi, eds. (North-Holland, Amsterdam, 1969), Chap. 4, pp. 181–239.